ELSEVIER

Physics Letters B 531 (2002) 119–126

PHYSICS LETTERS B

www.elsevier.com/locate/npe

Dipole coefficients in $B \to X_s\gamma$ in supersymmetry with large $\tan\beta$ and explicit CP violation

Müge Boz [a], Namık K. Pak [b]

[a] *Hacettepe University, Department of Physics, 06532 Ankara, Turkey*
[b] *Middle East Technical University, Department of Physics, 06531 Ankara, Turkey*

Received 10 January 2002; received in revised form 4 February 2002; accepted 8 February 2002

Editor: M. Cvetič

Abstract

We perform a detailed study of the electric and chromoelectric dipole coefficients in $B \to X_s\gamma$ decay in a supersymmetric scheme with explicit CP violation. In our analysis, we adopt the minimal flavor violation scheme by taking into account the $\tan\beta$-enhanced large contributions beyond the leading order. We show that the coefficients can deviate from the SM prediction significantly in both real and imaginary directions. Experimental bounds still allow for large deviations from the SM predictions for both dipole coefficients such that the CP asymmetry is as large as $\pm 8\%$. There are further implications of these coefficients for the charmless hadronic and semileptonic B decays. As a direct application of our analysis, we have discussed $\Lambda_b \to \Lambda\gamma$ decay.

© 2002 Elsevier Science B.V. Open access under CC BY license.

PACS: 11.30.Er; 11.30.Pb; 12.60.Jv; 13.25.Hw; 14.30.Ly

Keywords: Supersymmetry; $B \to X_s\gamma$ decay; Electric and chromoelectric dipole coefficients; Explicit CP violation

The Operator Product Expansion (OPE) combined with the heavy quark effective theory (HQET) forms the basic tool in analyzing the decays as well as productions of hadrons (see the review [1]). Basically, the effective Hamiltonian describing the scattering processes can be expanded in a series of local operators (whose hadronic matrix elements constitute the long-distance effects) with Wilsonian coefficients (which are generated by the short-distance effects). Among all the hadronic scattering processes the rare ones are particularly important, as the contributions of the standard electroweak theory (SM) and those of the 'new physics (NP)' arise at the same loop level thus suffering no relative loop suppressions. Furthermore, decays of the b-flavored hadrons (B, $B^\star$, Λ_b, ...), compared to strange and charmed ones, are especially important as for such systems the HQET is fully applicable, and via the OPE, one can both test the SM and search for possible NP effects, by confronting the associated Wilson coefficients with the experiment.

In this work we will analyze the electric and chromoelectric dipole coefficients (denoted hereafter by C_7 and C_8, respectively) describing the short-distance

E-mail address: muge@thep13.phys.hacettepe.edu.tr (M. Boz).

0370-2693/02 © 2002 Elsevier Science B.V. Open access under CC BY license.
PII: S0370-2693(02)01348-5

physics effects in rare B decays (e.g., $B \to X_s\gamma$, $B \to K^\star(892)\gamma$ and $B \to X_s\ell^+\ell^-, \ldots$) [2], by taking into account existing experimental results. The electric dipole coefficient C_7, rescaled to $\mu = m_b$ level, is directly constrained by the experimental result on $B \to X_s\gamma$ [3]. However, the situation for the coefficient C_8 is obscured by the fact that the gluonic decay $b \to sg$ is not directly accessible in experiments. However, this very coefficient plays an important role in the charmless hadronic B decays. For example, the theoretical predictions for the inclusive semileptonic decay rate $\Gamma(b \to ce\nu)$ and the charm multiplicity in B meson decays are significantly higher than the experimental results (see [4] and references therein). The most plausible solution to this discrepancy stems from possible enhancement of the chromoelectric coefficient C_8 by NP effects. Moreover, it is the relative phase between C_8 and C_7 which determines the CP asymmetry in $B \to X_s\gamma$, which will be measured in near-future B factories [5]. Consequently, it is essential to determine the size and phase of the gluonic coefficient in regions of the parameter space of NP where the theoretical predictions for $B \to X_s\gamma$ agrees with the experiment.

In what follows, we will take low-energy minimal supersymmetry (SUSY) with explicit CP violation as the NP candidate. We will adopt the minimal flavor violation scenario (MFV), take into account the $\tan\beta$-enhanced large contributions beyond the leading order (LO). The inclusive mode $B \to X_s\gamma$ has already been analyzed within such a scheme by [6] (in CP-conserving SUSY), and has been furthered by [7] to the CP-violating SUSY concluding a sizable CP asymmetry, which can compete with the experiment in near future. However, in both [6] and [7] the size and phase of C_8, its correlation with C_7, and its interdependence with the branching ratio, as well as its effects on the CP asymmetry have not been reported in detail. In particular, given the post-LEP bound on $\tan\beta \gtrsim 3.5$, it is necessary to have a detailed knowledge of C_8 in this portion of the SUSY parameter space. The main goal of this work is to determine the size and phase of the chromoelectric coefficient C_8 within the CP-violating SUSY at beyond-the-leading-order (BLO) precision in regions of the parameter space allowed by the existing $B \to X_s\gamma$ constraint.

The inclusive decay $B \to X_s\gamma$ is well approximated (within at most 10%) by the partonic decay $b \to s\gamma$ which is described by the effective Hamiltonian

$$H_{\rm eff} = -\frac{4G_F}{\sqrt{2}} V_{ts}^\star V_{tb} \sum_{i=1}^{8} C_i(\mu)\mathcal{O}_i(\mu)\,, \tag{1}$$

where V is the Cabibbo–Kobayashi–Maskawa (CKM) matrix, and the operator basis $\mathcal{O}_{i=1,\ldots,8}$ is defined in [2,8]. This OPE for the Hamiltonian separates the long-distance (the matrix elements of the local operators $\mathcal{O}_i$) and short-distance (associated Wilson coefficients C_i) at any scale $\mu \in (m_b, M_W)$. Moreover, HQET approximates the inclusive rate by the partonic one (all terms being of the order $\mathcal{O}(\Lambda_{\rm QCD}/m_b)$ and higher ones are negligible) [9].

Evolution of the Wilson coefficients from $\mu = M_W$ down to $\mu = m_b$ level is governed by the standard QCD RGEs:

$$\begin{aligned}
C_2(m_b) &= \frac{1}{2}\left(\eta^{-12/23} + \eta^{6/23}\right),\\
C_7(m_b) &= C_7(M_W)\eta^{16/23}\\
&\quad + C_8(M_W)\frac{8}{3}\left(\eta^{14/23} - \eta^{16/23}\right)\\
&\quad + C_2(M_W)\sum_{i=1}^{8} h_i\eta^{r_i},\\
C_8(m_b) &= C_8(M_W)\eta^{14/23} + C_2(M_W)\sum_{i=1}^{8} g_i\eta^{r_i},
\end{aligned} \tag{2}$$

where $\eta = \alpha_s(M_W)/\alpha_s(m_b)$, and the numerical coefficients h_i, r_i and g_i are given in [8].

The initial values for the QCD RGEs, $C_{2,7,8}(M_W)$, depend on details of the short-distance theory at $\mu \sim M_W$. In standard electroweak theory for instance, one finds $C_2(m_b) = 1.023$, $C_7(m_b) = -0.312$ and $C_8(m_b) = -0.148$ at BLO precision [2]. Consequently, the NP effects can appear in various ways: (i) there can be observable deviations from these numbers with or without sign change, or (ii) the coefficients can take complex values. Each type of departure from the SM prediction implies certain aspects of the weak-scale NP effects. For instance, for (ii), it is obvious that the NP brings new sources of CP violation, and necessarily, the CP asymmetry of the decay deviates from the SM prediction ($\lesssim 1\%$) [5,10].

In what follows, we will take SUSY with explicit CP violation as the NP candidate, and concentrate on

the results of [7] where the Wilson coefficients were computed at NLO precision for those threshold effects enhanced at large $\tan\beta$. Within this framework $C_2(M_W) = 1$ as in the SM, but the two dipole coefficients $C_{7,8}(M_W)$ are significantly modified compared to the LO results [11]. With the MFV scheme, only chargino–top squark, charged Higgs–top quark and W-boson–top quark loops give significant contributions

$$C_{7,8}(M_W) = C_{7,8}^{W}(M_W) + C_{7,8}^{H}(M_W) + C_{7,8}^{\chi}(M_W). \quad (3)$$

In CP-violating SUSY, at LO precision $C_{7,8}^{W,H}(M_W)$ are always real; they do not contribute to CP-violating observables, such as the CP-asymmetry, in the decay. However, the chargino contribution is complex due to the μ parameter (having finite phase ϕ_μ) and the stop trilinear coupling A_t (having finite phase ϕ_A) with approximate structure $e^{i(\phi_\mu+\phi_A)}$ [11].

With BLO precision, however, there are finite threshold corrections to each piece in (3) such that all three contributions $C_{7,8}^{W}(M_W)$, $C_{7,8}^{H}(M_W)$, $C_{7,8}^{\chi}(M_W)$ are now complex. Moreover, larger the $\tan\beta$ larger their imaginary parts, so that even naively one expects CP-violating effects to be enhanced at large $\tan\beta$. Indeed, as reported in [7], the BLO CP asymmetry is significantly larger than the LO one at sufficiently large $\tan\beta$. Although the asymmetry remains $\lesssim 8\%$ in both cases [12], there occurs an enhanced sensitivity to $\tan\beta$ for the BLO case.

In the following we will perform a numerical study of the electric and chromoelectric dipole coefficients, and discuss their phenomenological implications. In the numerical analysis, we take: (i) the light stop $\tilde{t}_2$ and the charged Higgs $H^\pm$ are degenerate and weight close to the weak scale, $M_{\tilde{t}_2} = M_H = 250$ GeV; (ii) the sfermions of first two generations are heavy enough, so that one can neglect their contribution to $B \to X_s\gamma$ (this is a viable way of suppressing the one-loop EDMs [7]); (iii) the SU(2) gaugino, the right-handed sbottom and the heavy stop are heavy, $M_2 = M_{\tilde{t}_1} = \widetilde{m}_{b_R} = 1$ TeV, and form the SUSY breaking scale; (iv) the stop and sbottom trilinear couplings have the same phase, $\theta_{A_b} = \theta_{A_t}$, and the latter is degenerate with the μ parameter $|\mu| = |A_b| = 150$ GeV (sbottom parameters are needed for 2-loop EDM calculations [13]); and finally (v) the light stop is dominantly right-handed to agree with the electroweak precision data, hence the stop mixing is to be sufficiently small ($\theta_{\tilde{t}} = \pi/20$). Moreover, we vary $\tan\beta$ from 10 to 50 and the phase $\phi_{A,\mu}$ from 0 to π in forming the scatter plots. The parameter space mentioned here has been determined after trying several combinations, and it is one those points yielding large CP-violation in the system. One particularly notices that the lightest chargino is a Higgsino so that CP-violation via chargino–stop contribution is enhanced. In minimal supergravity, for instance, the lightest chargino is SU(2) gaugino and thus CP-violation is very much suppressed.

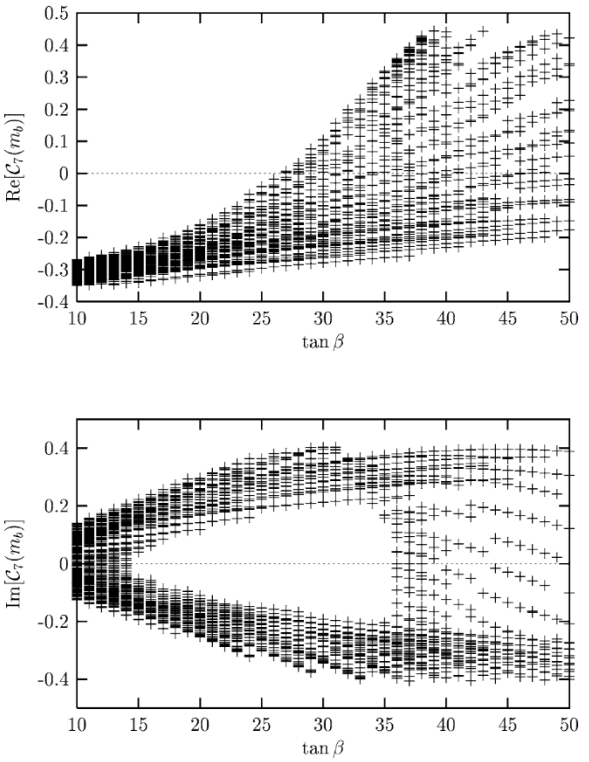

Fig. 1. The $\tan\beta$ dependence of Re[$\mathcal{C}_7(m_b)$] (upper window) and Im[$\mathcal{C}_7(m_b)$] (lower window), for the values of ϕ_μ and ϕ_A varying from 0 to π.

Depicted in Fig. 1 is the $\tan\beta$ dependence of Re[$\mathcal{C}_7(m_b)$] and Im[$\mathcal{C}_7(m_b)$] for $10 \leqslant \tan\beta \leqslant 50$ and $0 \leqslant \phi_\mu, \phi_A \leqslant \pi$. When $\tan\beta \gtrsim 10$, Re[$\mathcal{C}_7(m_b)$] is close to the SM value and Im[$\mathcal{C}_7(m_b)$] is evenly distributed around the origin, being consistent with zero. However, as $\tan\beta$ rises towards larger values, so does Re[$\mathcal{C}_7(m_b)$], crossing zero around $\tan\beta \sim 27$.

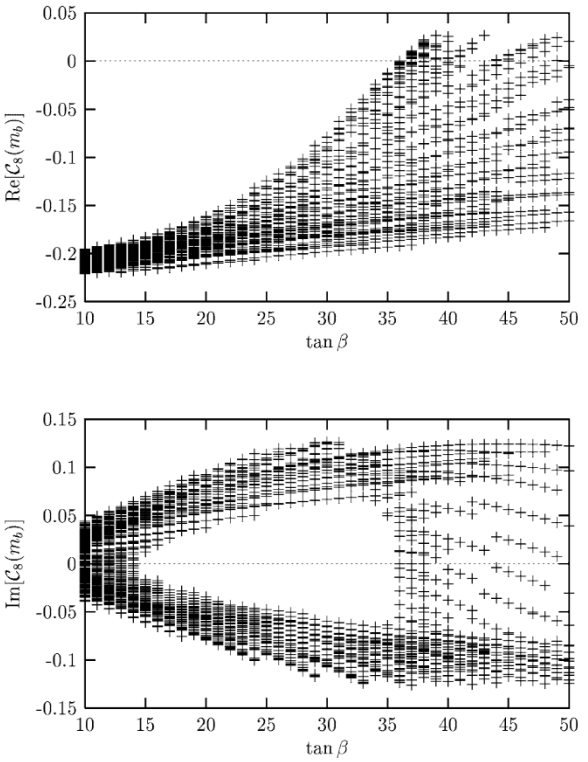

Fig. 2. The $\tan\beta$ dependence of $\mathrm{Re}[\mathcal{C}_8(m_b)]$ (upper window) and $\mathrm{Im}[\mathcal{C}_8(m_b)]$ (lower window), for the values of ϕ_μ and ϕ_A varying from 0 to π.

When $\tan\beta \gtrsim 27$, $\mathrm{Re}[\mathcal{C}_7(m_b)]$ takes both negative and positive values, and it can be as large as 0.4. The imaginary part of $\mathcal{C}_7$, however, rises with increasing $\tan\beta$ in absolute magnitude for both negative and positive directions in an approximately symmetric manner. For $\tan\beta \gtrsim 35$, its distribution is levelled with a value swinging between -0.35 and $+0.35$ smoothly. Clearly, for large enough $\tan\beta$ there are regions of the parameter space where $\mathrm{Im}[\mathcal{C}_7(m_b)]$ is not consistent with zero, signalling therefore a clear sign of the NP effects. An approximate expression valid for large $\tan\beta$ can be given as $\mathcal{C}_7 \sim 0.4\, e^{\pm i\pi/4}$, which is far away from the SM prediction in both size and phase. However, there are regions of the parameter space where $\mathcal{C}_7$ is pure imaginary, is pure real or vanishes exactly.

Similar to observations made for Fig. 1, one can discuss the Wilson coefficient $\mathcal{C}_8$ using Fig. 2 where its real (upper window) and imaginary (lower window) parts are separately plotted against $\tan\beta$ when

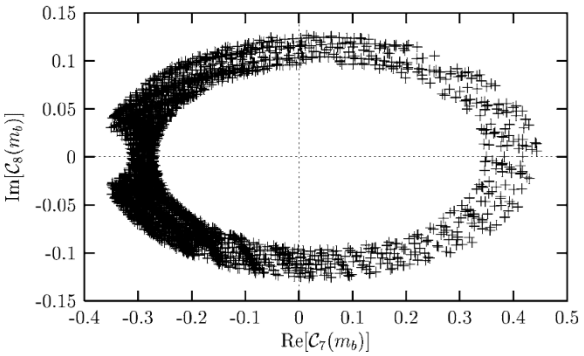

Fig. 3. Dependence of $\mathrm{Im}[\mathcal{C}_8(m_b)]$ on $\mathrm{Re}[\mathcal{C}_7(m_b)]$. The width of the ellipsoid corresponds to present experimental accuracy for $\mathrm{BR}(B \to X_s\gamma)$.

$\phi_{\mu,A}$ vary from 0 to π. One notices that, unlike $\mathcal{C}_7$, for low $\tan\beta$, $\mathrm{Re}[\mathcal{C}_8(m_b)]$ deviates from its SM value. This stems from the fact that $\mathcal{C}_8(m_b)$ is directly proportional to $\mathcal{C}_8(M_W)$ (up to small corrections proportional to $\mathcal{C}_2(M_W)$), and, therefore, the NP effects at short distances are directly reflected to the hadronic scale. As $\tan\beta$ rises to larger values, both $\mathrm{Re}[\mathcal{C}_8(m_b)]$ and $\mathrm{Im}[\mathcal{C}_8(m_b)]$ gradually increase where the former crosses zero around $\tan\beta \sim 35$. In large $\tan\beta$ regime, $\mathrm{Re}[\mathcal{C}_8(m_b)]$ can take positive values only in a small portion of the parameter space whereas $\mathrm{Im}[\mathcal{C}_8(m_b)]$ swings between -0.1 and 0.1 almost evenly. One notices that, as in $\mathcal{C}_7$, in certain regions of the parameter space $\mathcal{C}_8(M_W)$ can be pure real, pure imaginary or just vanish. Those points where both $\mathcal{C}_7$ and $\mathcal{C}_8$ vanish are particularly interesting, as in this case one has to saturate the experimental bounds on $B \to X_s\gamma$ via the chirality-flipped Wilson coefficients, implying large contributions due to the gluino exchange [14]. As we are working in the MFV scheme, such effects are obviously beyond the scope of our discussion.

Depicted in Fig. 3 is the dependence of $\mathrm{Im}[\mathcal{C}_8(m_b)]$ on $\mathrm{Re}[\mathcal{C}_7(m_b)]$. Here the size and shape of the ellipsoidal region is determined by the accuracy of the experimental results on $\mathrm{BR}(B \to X_s\gamma)$. The main NP effect occurs in pushing $\mathrm{Re}[\mathcal{C}_7(m_b)]$ to larger values compared to the SM prediction instead of smaller ones. The small region around $\mathrm{Re}[\mathcal{C}_7(m_b)] \sim -0.3$ corresponds to the SM validity domain where imaginary parts of both coefficients remain around zero.

Fig. 4 illustrates the dependence of $A_{\mathrm{CP}}(B \to X_s\gamma)$ on $\mathrm{Re}[\mathcal{C}_8(m_b)]$ (upper window), and on

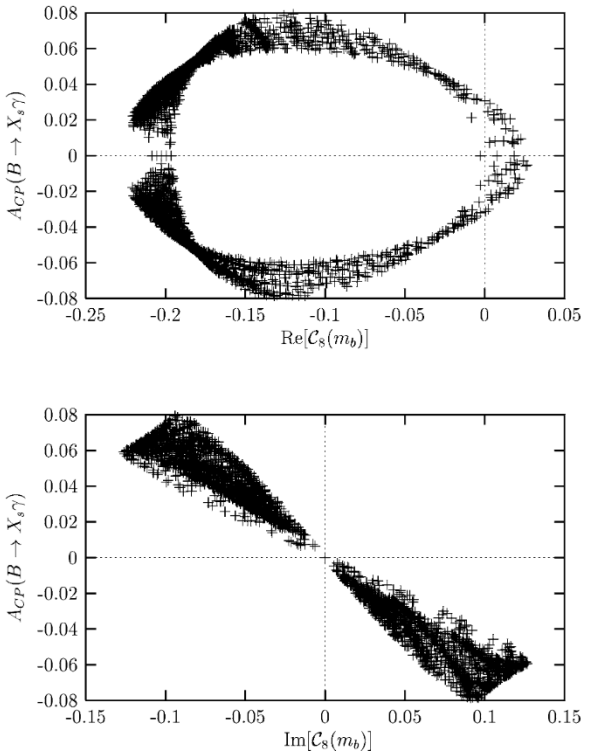

Fig. 4. The dependence of $A_{\mathrm{CP}}(B \to X_s\gamma)$ on $\mathrm{Re}[\mathcal{C}_8(m_b)]$ (upper window) and on $\mathrm{Im}[\mathcal{C}_8(m_b)]$ (lower window).

$\mathrm{Im}[\mathcal{C}_8(m_b)]$ (lower window). As we can see from the upper window, the asymmetry takes the largest value $\pm 8\%$ when $\mathrm{Re}[\mathcal{C}_8(m_b)]$ is in the range of the SM prediction for $\mathcal{C}_8(m_b)$. One notes that in a more general model CP asymmetry can be as large as 20% [10]. Moreover, in certain small corners of the SUSY parameter space the CP asymmetry can be enhanced by a factor of 2 [15]. When $\mathrm{Re}[\mathcal{C}_8(m_b)]$ takes larger or smaller values than the SM prediction, the asymmetry gradually drops to the corresponding SM prediction $\sim 1\%$. The dependence of the CP asymmetry on $\mathrm{Im}[\mathcal{C}_8(m_b)]$, however, shows that the maximal values are attained when $\mathrm{Im}[\mathcal{C}_8(m_b)] \sim \pm 0.1$, which is far away from the SM prediction. In conclusion, the asymmetry is roughly an order of magnitude larger than what is expected in the SM, and this happens when $\mathrm{Re}[\mathcal{C}_8(m_b)]$ remains close to the SM prediction, and $\mathrm{Im}[\mathcal{C}_8(m_b)]$ is large and has a similar size as the real part.

A closer comparative look at the figures suggests that the CP asymmetry, which will be measured in near-future B factories with increasing precision, is maximal when $|\mathcal{C}_8(m_b)| \sim |\mathcal{C}_7(m_b)|$. This results confirms earlier predictions [16], where it was already shown that $A_{\mathrm{CP}}(B \to X_s\gamma) \sim 10\%\ |\mathcal{C}_8(m_b)/\mathcal{C}_7(m_b)|$.

Even after including the NLL corrections to the semileptonic inclusive B decay $B \to Xe\nu$, the theoretical predictions for the branching ratio and the charm multiplicity turn out to be larger than the experimental result [4,17]. Therefore, it is conceivable that possible enhancements in $\mathcal{C}_8$ can account for the existing discrepancy between the theory and the experiment. As the numerical analyses above show, it is possible to significantly shift this coefficient in both real and imaginary directions compared to the SM prediction. Therefore, the experimental result on $B \to X_s\gamma$ allows for large deviations in chromoelectric as well as electric coefficients at large values of $\tan\beta$, where the SUSY threshold corrections are important. Concerning the semileptonic B decays, the exclusive channel $B \to X_s\ell^+\ell^-$ is another example having both theoretical and experimental importance. This follows from the fact that the forward–backward asymmetry A_{FB} of this decay vanishes at a specific value of the dilepton invariant mass [18] in a hadronically clean way. This zero of A_{FB} occurs at the point $m_{\ell\ell}^2 \sim -m_b^2\ \mathrm{Re}[\mathcal{C}_7(m_b)/\mathcal{C}_9(m_b)]$ where $\mathcal{C}_9(m_b)$ is the four-fermion operator coefficient (not computed here). The important point is that the position of the zero shifts in accord with the NP contributions to the Wilson coefficients. Suppose that $\mathcal{C}_7(m_b)$ alone is shifted in complex direction, then it is clear that the critical value of the dilepton mass $m_{\ell\ell}^2$ is shifted back and forth, depending on the parameter values [18].

There are other processes where the radiatively corrected Wilson coefficients play an important role. As an application, for instance, we analyze the bottom baryon radiative decay, $\Lambda_b \to \Lambda\gamma$, which is again dominated by the mechanism $b \to s\gamma$. We will particularly concentrate on the dependence of the branching ratio on the Wilson coefficients at the weak scale.

The decay rate of $\Lambda_b \to \Lambda\gamma$ has been computed in [19], and its expression is given by:

$$\Gamma(\Lambda_b \to \Lambda\gamma) = \frac{1}{8\pi}\left(\frac{m_{\Lambda_b}^2 - m_{\Lambda}^2}{m_{\Lambda_b}}\right)^3 \times \left(|a|^2 + |b|^2\right), \tag{4}$$

with

$$a = \frac{G_F}{\sqrt{2}}\frac{e}{8\pi^2}2C_7(m_b)m_b V_{tb}V_{ts}^* \times \left(f_1^{\Lambda\Lambda_b}(0) - f_2^{\Lambda\Lambda_b}(0)\right),$$

$$b = \frac{G_F}{\sqrt{2}}\frac{e}{8\pi^2}2C_7(m_b)m_b V_{tb}V_{ts}^* \times \left(g_1^{\Lambda\Lambda_b}(0) + \left(\frac{m_{\Lambda_b} - m_\Lambda}{m_{\Lambda_b} + m_\Lambda}\right)g_2^{\Lambda\Lambda_b}(0)\right). \quad (5)$$

The form factors in a and b coefficients, depend on the momentum transfer as follows [19,20]:

$$f_i(q^2) = f_i\left(q_m^2\right)\left(\frac{1 - q_m^2/m_V^2}{1 - q^2/m_V^2}\right)^n,$$

$$g_i(q^2) = g_i\left(q_m^2\right)\left(\frac{1 - q_m^2/m_A^2}{1 - q^2/m_A^2}\right)^n, \quad (6)$$

where $q_m^2 = (m_{\Lambda_b} - m_\Lambda)^2$ and, $q^2 = p_{\Lambda_b} - p_\Lambda$, with $n = 1$ and $n = 2$ representing the monopole and dipole contributions. Here, m_V and m_A are the pole masses of the vector and axial vector mesons, respectively.

In the numerical analysis, following [19,20], we let $f_1^{\Lambda\Lambda_b}(q_m^2) = g_1^{\Lambda\Lambda_b}(q_m^2) = 0.64$, $g_2^{\Lambda\Lambda_b}(q_m^2) = -0.10$, and $f_2^{\Lambda\Lambda_b}(q_m^2) = -0.31$ for the values of the heavy–light form factors. Additionally, we take $m_b(m_b) = 4.25$ GeV, $m_{\Lambda_b} = 5.624$ GeV, $m_V = 5.42$ GeV, $m_A = 5.86$ GeV, and $\tau(\Lambda_b) = 1.23 \times 10^{-12}$ s. In forming the scatter plots, we vary $\tan\beta$ from 10 to 50 and the phase $\phi_{A,\mu}$ from 0 to π.

Depicted in Fig. 5 is the dependence of the branching ratio of $\Lambda_b \to \Lambda\gamma$ ($\mathcal{B}(\Lambda_b \to \Lambda\gamma)$) on $\mathrm{Re}[\mathcal{C}_8(M_W)]$ (upper window) and $\mathrm{Im}[\mathcal{C}_7(M_W)]$ (lower window), for $10 \leqslant \tan\beta \leqslant 50$ and $0 \leqslant \phi_\mu, \phi_A \leqslant \pi$, where only the monopole q^2 dependence for baryon form factors is considered ($n = 1$). As is seen from both windows, $\mathrm{Re}[\mathcal{C}_8(M_W)]$ takes negative values up to $\mathcal{B}(\Lambda_b \to \Lambda\gamma) \sim 1.7 \times 10^{-5}$, whereas $\mathrm{Im}[\mathcal{C}_8(M_W)]$ is evenly distributed around the origin in this interval. $\mathrm{Re}[\mathcal{C}_8(M_W)]$ starts to take both positive and negative values, when $\mathcal{B}(\Lambda_b \to \Lambda\gamma) \gtrsim 1.7 \times 10^{-5}$. It can take only positive values for $\mathcal{B}(\Lambda_b \to \Lambda\gamma) \gtrsim 2.7 \times 10^{-5}$, and can be as large as ~ 0.2. On the other hand, for $\mathcal{B}(\Lambda_b \to \Lambda\gamma) \gtrsim 1.7 \times 10^{-5}$, $\mathrm{Im}[\mathcal{C}_8(M_W)]$ increases in both positive and negative directions in a symmetric manner. Clearly, there are certain regions of the parameter space where $\mathcal{C}_8(M_W)$ can be pure real, pure imaginary as well as it just vanishes.

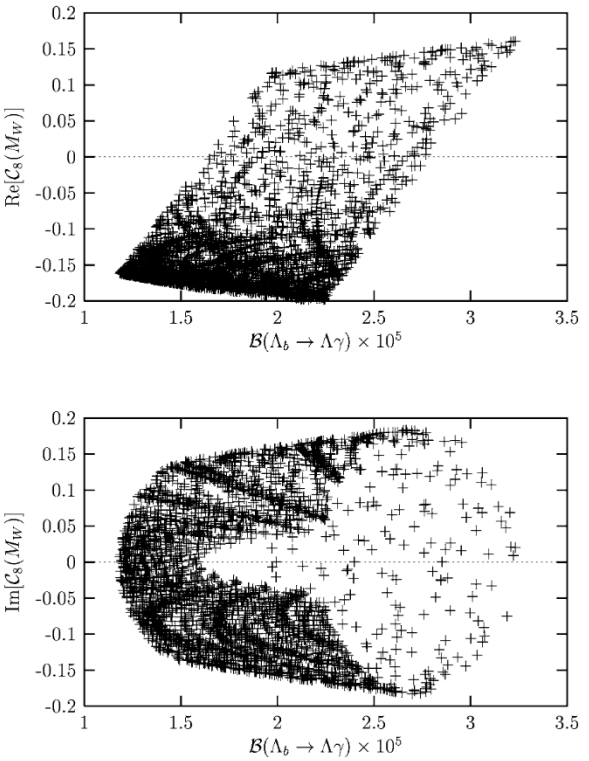

Fig. 5. The dependence of $\mathcal{B}(\Lambda_b \to \Lambda\gamma)$ on $\mathrm{Re}[\mathcal{C}_8(M_W)]$ (upper window) and on $\mathrm{Im}[\mathcal{C}_8(M_W)]$ (lower window), for the values of ϕ_μ and ϕ_A varying from 0 to π.

In the recent work [19], it has been shown that $\mathcal{B}(\Lambda_b \to \Lambda\gamma)$ has a magnitude of 1.9×10^{-5}, when only the monopole q^2 dependence of the baryon form factors is considered ($n = 1$). This decay has also been considered in [21] with the predicted branching ratios in the range of $(1.2\text{–}1.9) \times 10^{-5}$. As one can see from both windows of Fig. 5, $\mathcal{B}(\Lambda_b \to \Lambda\gamma)$ varies in the range of $(1\text{–}3.2) \times 10^{-5}$, and the maximal values of $\mathcal{B}(\Lambda_b \to \Lambda\gamma)$ are attained when $\mathrm{Re}[\mathcal{C}_8(M_W)] \sim 0.2$, and $\mathrm{Im}[\mathcal{C}_8(M_W)] \sim \pm 0.2$, which are away from the SM prediction for $\mathcal{C}_8(M_W)$. A closer comparative look at the figure suggests that when $\mathcal{C}_8(M_W)$ is in the range of the SM prediction, for instance, $\mathcal{C}_8(M_W) = -0.086$ [8], $\mathcal{B}(\Lambda_b \to \Lambda\gamma)$ drops nearly to $\sim 1.9 \times 10^{-5}$, which is consistent with the results of SM [19]. However, one notes that at this particular value of the branching ratio, there are other solutions in the parameter space where $\mathcal{C}_8(M_W)$ can deviate from its SM value not only in sign, but also in magnitude, as it can be complex.

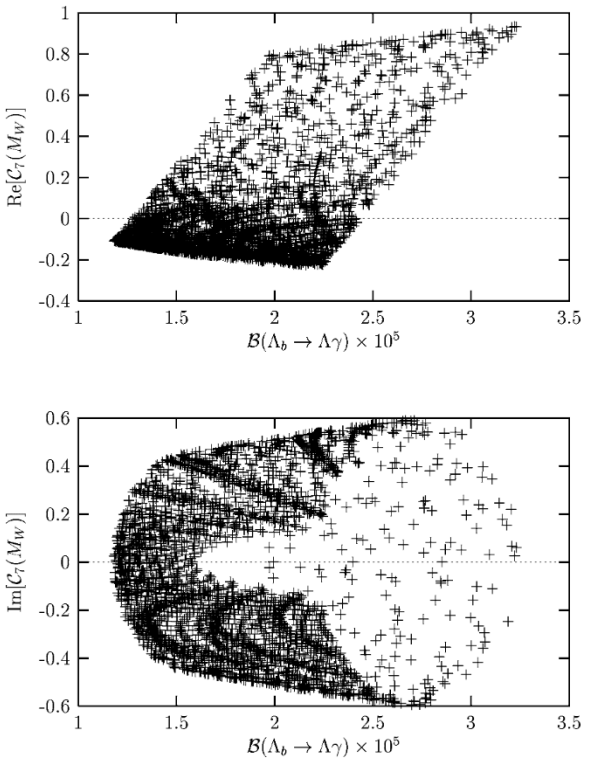

Fig. 6. The dependence of $\mathcal{B}(\Lambda_b \to \Lambda\gamma)$ on Re[$\mathcal{C}_7(M_W)$] (upper window) and on Im[$\mathcal{C}_7(M_W)$] (lower window), for the values of ϕ_μ and ϕ_A varying from 0 to π.

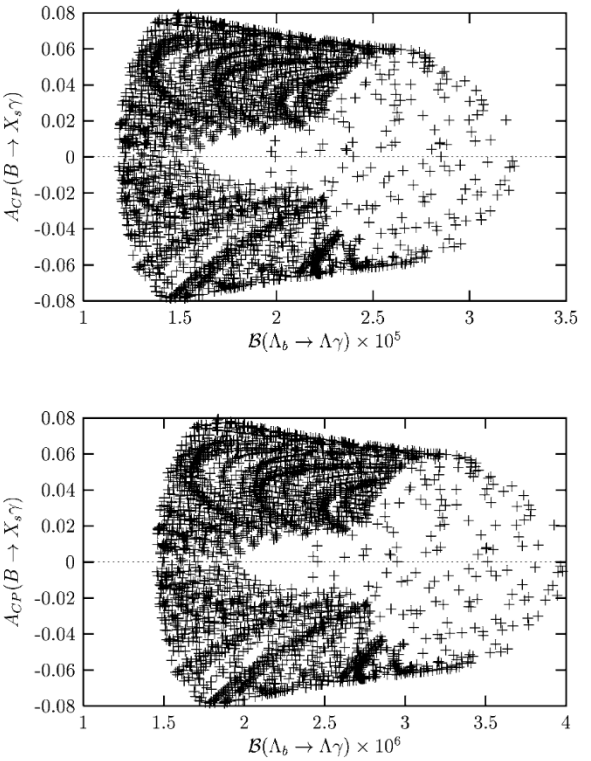

Fig. 7. The dependence of $\mathcal{B}(\Lambda_b \to \Lambda\gamma)$ on $A_{\rm CP}(B \to X_s\gamma)$ for $n = 1$ (upper window) and for $n = 2$ (lower window).

We would like to note that the analysis of [19] has been carried out in the context of the SM, and $C_7(m_b)$ has a fixed value ($C_7(m_b) = -0.312$). However, in our work, C_7 and C_8 are complex, and as we have shown in Figs. 1 and 2, they vary in a wider range. For instance, approximate expressions of $C_{7(8)}$ valid for large $\tan\beta$ can be given as $\mathcal{C}_7 \sim 0.4\, e^{\pm i\pi/4}$, and $\mathcal{C}_8 \sim 0.1\, e^{\pm i\pi/4}$, which are far away from the SM predictions in both size and phase. Therefore, having a wide range of parameter space, the model under concern gives new allowed regions. It is natural that there are regions in the parameter space where our prediction for $\mathcal{B}(\Lambda_b \to \Lambda\gamma)$ agrees with that of SM.

Similar to the observations made for Fig. 5, one can discuss the Wilson coefficient $\mathcal{C}_7$ using Fig. 6, where its real (upper window) and imaginary (lower window) parts are separately plotted against $\mathcal{B}(\Lambda_b \to \Lambda\gamma)$, when $\phi_{\mu,A}$ vary from 0 to π, and only monopole contribution is considered ($n = 1$). As $\mathcal{B}(\Lambda_b \to \Lambda\gamma)$ rises to larger values, both Re[$\mathcal{C}_7(M_W)$] and Im[$\mathcal{C}_7(M_W)$] gradually increase, where the former crosses zero around $\mathcal{B}(\Lambda_b \to \Lambda\gamma) \sim 1.3 \times 10^{-5}$. Re[$\mathcal{C}_7(M_W)$] starts to take positive values only when $\mathcal{B}(\Lambda_b \to \Lambda\gamma) \gtrsim 2.4 \times 10^{-5}$, whereas Im[$\mathcal{C}_7(M_W)$] swings between ± 0.6. Like $\mathcal{C}_8$, there are observable deviations from the SM prediction with or without sign change, and it can take complex values as well. However, a comparative glance at the figure shows that, when $\mathcal{C}_7(M_W)$ is in the range of the SM prediction, for instance $\mathcal{C}_7(M_W) = -0.161$ [8], $\mathcal{B}(\Lambda_b \to \Lambda\gamma) \sim 1.3 \times 10^{-5}$, which is close to the SM value [19,21].

Depicted in Fig. 7 is the dependence of $\mathcal{B}(\Lambda_b \to \Lambda\gamma)$ on $A_{\rm CP}(B \to X_s\gamma)$, when only the monopole (upper window) and the dipole (lower window) q^2 dependences are considered. As is noticed from the upper and lower windows $\mathcal{B}(\Lambda_b \to \Lambda\gamma)$ is of the orders of 10^{-5} and 10^{-6}, for the monopole ($n = 1$) and dipole ($n = 2$) contributions, respectively. In both cases $\mathcal{B}(\Lambda_b \to \Lambda\gamma)$ behave similarly. However, it decreases by an order of magnitude in the dipole

case, and the maximal values of $A_{CP}(B \to X_s\gamma)$ are obtained when $\mathcal{B}(\Lambda_b \to \Lambda\gamma) \sim 1.5 \times 10^{-5}$ (1.9×10^{-6}) for $n = 1$ ($n = 2$). In the recent work of [19], it has been shown that $\mathcal{B}(\Lambda_b \to \Lambda\gamma) = 2.3 \times 10^{-6}$ for $n = 2$. As we can see from the upper and lower windows, the asymmetry nearly takes the largest value, when $\mathcal{B}(\Lambda_b \to \Lambda\gamma)$ is in the range of the SM prediction [19,22,23]. When $\mathcal{B}(\Lambda_b \to \Lambda\gamma)$ takes larger values than the SM prediction, the asymmetry gradually drops to the corresponding SM prediction $\sim 1\%$.

In conclusion, we have computed the dipole coefficients $C_{7,8}$ in SUSY with explicit CP violation with special emphasis on large values of $\tan\beta$. We have shown that the present experimental bounds on $B \to X_s\gamma$ allows for large deviations in the Wilson coefficients (with respect to the SM prediction) in both real and imaginary directions. The CP asymmetry in the decay is enhanced by an order of magnitude, thanks to especially the SUSY threshold corrections. The allowed deviations from the SM values can account for (being a plausible hypothesis) the discrepancy between the experiment and theory for the semileptonic B decays. As an illustration, we have discussed $\Lambda_b \to \Lambda\gamma$ decay.

Acknowledgements

M.B. would like to thank the Scientific and Technical Research Council of Turkey (TÜBİTAK) for partial support under the project, No. TBAG2002 (100T108).

References

[1] B. Chibisov, R.D. Dikeman, M.A. Shifman, N. Uraltsev, Int. J. Mod. Phys. A 12 (1997) 2075, hep-ph/9605465;
M.A. Shifman, hep-ph/9510377.
[2] K. Chetyrkin, M. Misiak, M. Munz, Phys. Lett. B 400 (1997) 206;
K. Chetyrkin, M. Misiak, M. Munz, Phys. Lett. B 425 (1997) 414, hep-ph/9612313, Erratum.
[3] R. Barate et al., ALEPH Collaboration, Phys. Lett. B 429 (1998) 169;
S. Ahmed et al., CLEO Collaboration, hep-ex/9908022;
K. Abe et al., Belle Collaboration, Phys. Lett. B 511 (2001) 151, hep-ex/0103042.
[4] T. Besmer, C. Greub, T. Hurth, Nucl. Phys. B 609 (2001) 359, hep-ph/0105292.
[5] A.L. Kagan, M. Neubert, Eur. Phys. J. C 7 (1999) 5, hep-ph/9805303.
[6] G. Degrassi, P. Gambino, G.F. Giudice, JHEP 0012 (2000) 009, hep-ph/0009337;
M. Carena, D. Garcia, U. Nierste, C.E. Wagner, Phys. Lett. B 499 (2001) 141, hep-ph/0010003.
[7] D.A. Demir, K.A. Olive, Phys. Rev. D 65 (2002) 034007, hep-ph/0107329.
[8] A.J. Buras, M. Misiak, M. Munz, S. Pokorski, Nucl. Phys. B 424 (1994) 374, hep-ph/9311345.
[9] R.D. Dikeman, M.A. Shifman, N.G. Uraltsev, Int. J. Mod. Phys. A 11 (1996) 571, hep-ph/9505397.
[10] A.L. Kagan, M. Neubert, Phys. Rev. D 58 (1998) 094012, hep-ph/9803368.
[11] S. Bertolini, F. Borzumati, A. Masiero, G. Ridolfi, Nucl. Phys. B 353 (1991) 591;
H. Baer, M. Brhlik, D. Castano, X. Tata, Phys. Rev. D 58 (1998) 015007, hep-ph/9712305.
[12] F.M. Borzumati, C. Greub, Phys. Rev. D 58 (1998) 074004, hep-ph/9802391;
M. Aoki, G.C. Cho, N. Oshimo, Nucl. Phys. B 554 (1999) 50, hep-ph/9903385.
[13] D. Chang, W. Keung, A. Pilaftsis, Phys. Rev. Lett. 82 (1999) 900, hep-ph/9811202;
A. Pilaftsis, Phys. Lett. B 471 (1999) 174, hep-ph/9909485;
D. Chang, W. Chang, W. Keung, Phys. Lett. B 478 (2000) 239, hep-ph/9910465.
[14] L. Everett, G.L. Kane, S. Rigolin, L.T. Wang, T.T. Wang, JHEP 0201 (2002) 022, hep-ph/0112126.
[15] S.W. Baek, P. Ko, Phys. Rev. Lett. 83 (1999) 488, hep-ph/9812229.
[16] L. Wolfenstein, Y.L. Wu, Phys. Rev. Lett. 73 (1994) 2809, hep-ph/9410253;
T.M. Aliev, D.A. Demir, E. Iltan, N.K. Pak, Phys. Rev. D 54 (1996) 851, hep-ph/9511352.
[17] E. Bagan, P. Ball, V.M. Braun, P. Gosdzinsky, Phys. Lett. B 342 (1995) 362;
E. Bagan, P. Ball, V.M. Braun, P. Gosdzinsky, Phys. Lett. B 374 (1995) 363, hep-ph/9409440, Erratum.
[18] A. Ali, P. Ball, L.T. Handoko, G. Hiller, Phys. Rev. D 61 (2000) 074024, hep-ph/9910221;
G. Burdman, Phys. Rev. D 57 (1998) 4254, hep-ph/9710550.
[19] H.Y. Cheng, K.C. Yang, hep-ph/0201015.
[20] H.Y. Cheng, Phys. Rev. D 56 (1997) 2799, hep-ph/9612223.
[21] H.Y. Cheng, C.Y. Cheung, G.L. Lin, Y.C. Lin, T.M. Yan, H.L. Yu, Phys. Rev. D 51 (1995) 1199, hep-ph/9407303.
[22] H.Y. Cheng, B. Tseng, Phys. Rev. D 53 (1996) 1457;
H.Y. Cheng, B. Tseng, Phys. Rev. D 55 (1996) 1697, hep-ph/9502391, Erratum.
[23] P. Singer, D.X. Zhang, Phys. Lett. B 383 (1996) 351, hep-ph/9606343;
R. Mohanta, A.K. Giri, M.P. Khanna, M. Ishida, S. Ishida, Prog. Theor. Phys. 102 (1999) 645, hep-ph/9908291.